

Thermodynamic studies of hydrated metal oxide precipitate for the removal of fluoride from water

Hari Paudyal*, Bimala Pageni**, Kedar Nath Ghimire* and Katsutoshi Inoue***

*Central Department of Chemistry, Tribhuvan University, Kirtipur, Kathmandu, Nepal.

**Department of Botany, Trichandra Multiple Campus, Ghantaghar, Kathmandu, Nepal.

***Department of Applied Chemistry, Saga University, Honjo 1, Saga, 840-8502, Japan.

Abstract: Hydrated tri metal oxide (HTMO) precipitate is investigated using a mixed solution containing cerium, aluminum, and titanium by precipitation for fluoride ion removal from water. PZC for the investigated HTMO precipitate is determined to be 6.5 from pH drift method. Fluoride adsorption by HTMO precipitate is pH dependent, with adsorption rates of more than 98 percent occurring at pH 2.3 to 6.7. The highest solid phase distribution of fluoride is observed at pH around 6. Fluoride adsorption onto HTMO precipitate increased with temperature, implying that the adsorption reaction is endothermic, as evidenced by the positive value of ΔH° calculated from the thermodynamic calculations. The spontaneous process is indicated by a negative ΔG° value for all temperatures. The fluoride adsorption rate onto this adsorbent is rapid, and equilibrium is reached in less than four hours. An alkali (NaOH) solution effectively desorbed fluoride from a fluoride-loaded HTMO precipitate. As a result, the HTMO precipitate studied in this work is expected to be a viable as fluoride-removing material from water.

Keywords: Desorption; Fluoride adsorption; HTMO precipitate; Point of zero charge (PZC); Spontaneous and endothermic.

Introduction

Water is very important requirements for the life of plants and animals on the earth. We cannot imagine our life without water in earth. Nowadays the quality of surface and ground water on the earth is degrading because of both natural and manmade activities¹. Contamination of water with fluoride is emerging issues these days because of its adverse effect to our bone tissue². Naturally, the pollution water with fluoride occurs due to the weathering of fluoride rich rocks and minerals whereas anthropogenic pollution occurs due to the discharge of waste water produced from plating, toothpaste, semiconductor production, and production of fluoride-rich pesticides^{3, 4}. Trace amount of fluoride is essential for the strengthening of our dental

carries whereas excess concentration of fluoride is detrimental and invites various health issues including dental and skeletal fluorosis, kidney damage, neurological disorders, and infertility in male and endocrinal disorder³. Because of such an adverse effect of fluoride, the World Health Organization (WHO) set the maximum acceptable level of 1.5 mg/L fluoride in drinking water⁵. Thus, the excess concentration of fluoride in water should be removed before discharging into the portable water bodies. Some methods such as precipitation⁶, co-precipitation⁷, reverse osmosis/nanofiltration⁸, electro-dialysis⁹, and ion exchange¹⁰ have been practiced for the removal of fluoride ion from water. Literature shows that high concentration of fluoride can be commonly treated by precipitation

Author for correspondence: Hari Paudyal, Central Department of Chemistry, Tribhuvan University, Kathmandu, Nepal.
Email: haripaudyal9@gmail.com

Received: 01 Mar 2022; First Review: 18 Mar 2022; Second Review: 31 Mar 2022; Accepted: 02 Apr 2022.
Doi: <https://doi.org/10.3126/sw.v15i15.45849>

techniques using lime water as precipitating materials. Although lime precipitation is effective for the treatment of water containing high concentration of fluoride ion however the treated water leaves the residual fluoride in the range of 10 -12 mg/L due to solubility limit of CaF_2 which needs further processing and treatment to meet legal standard.

Trace amount of fluoride remains after lime precipitation is generally treated by co-precipitation with aluminum salts or alum, and using commercial ion exchange resins. Co-precipitation with aluminum salts/or alum produces large amount of sludge containing huge amount of water which also needs further dewatering and treatment for excessive amount of aluminum. Although the techniques such as reverse osmosis, electro-dialysis, nano-filtration and membrane separation are effective for the fluoride ion removal however their applications are amid due to their high operating cost and necessities of technical manpower. Ion exchange method can selectively remove fluoride ion to less than 1.5 mg/L but the application of a plastic based ion exchange resins for water treatment is limited because of their long chemical synthetic route, and expensive for water treatment. Furthermore, it also invites another trouble of managing spent resin obtained after fluoride treatment due to non-degradable behaviors. On the other hand, the metal loaded adsorbents such as modified ceria nanoparticles, metal loaded starch, magnetic modified activated carbon, FeCl_3 modified activated carbon, and Zr (IV) loaded pomegranate effective due to their high potential and selectivity¹¹⁻¹⁵. Nowadays, metal oxide/hydroxide-based ion exchangers are considered to be a emerging promising materials for the water treatment because of their very popular and effective due to ease of synthesis, high degree of selectivity and higher ion exchange capacity.

In the present work, metal oxide/hydroxide-based adsorbent is prepared by precipitation of titanium aluminum and iron with caustic soda. Main objective of this current research is to fabricate the new metal oxide/hydroxide based composite material and explore its ability for the removal of trace level of fluoride ion from aqueous solution. To this

purpose, the fluoride removal behavior of investigated HTMOPin terms of different adsorption parameters such as pH, contact time, concentration, adsorbent dose is systematically studied together with desorption behavior in batch mode in this work.

Materials and method

Chemicals and instruments

All the chemicals employed in this study were of analytical grade chemicals and used without further purification. Stock and working solutions were prepared using de-ionized water. Fluoride standard solution (1000 mg/L) for ICS calibrations was purchased from Sigma Aldrich, Co. Ltd., Japan. Sodium fluorides (NaF), sodium hydroxide (NaOH), and hydrochloric acid (HCl) were purchased from Wako Chemicals Co. Ltd., Japan. The working solutions were freshly prepared by diluting the stock solution at the time of experiments. The pH meter (HM-30R, DKK-TOA Corporation, Japan) was used to measure the pH of the solution. The concentrations of fluoride before and after adsorption were measured by using ion chromatography (Dionex ICS-1500, Conquer Scientific, USA).

Synthesis of HTMO precipitates

Hydrated metal oxide-based adsorbent for fluoride ion removal was prepared by precipitation of metal solution. Fifty milliliter of aluminum chloride (AlCl_3), cerium chloride (CeCl_3) and ferric chloride (FeCl_3) solutions (each having 0.1M concentrations) were mixed homogeneously using magnetic stirrer at room temperature. After that, 5M NaOH solution was added drop wise from burette with gentle stirring until pH 8.5 for complete precipitation of all three metal ions. The precipitated mixture was placed in an oven at 343K overnight for ageing then it was filtered. The residue was collected and washed several times with distilled water until neutral pH and finally dried at 423K for 48 hours. The dry product obtained in this way is termed as hydrated tri metal oxide precipitate and here forth abbreviated as HTMO precipitate which is used for the adsorption of fluoride ion at the time of experiment.

Batch wise study

In the batch studies, the 100mL Erlenmeyer flasks containing 15 mg of the HTMO precipitates and 10 mL of fluoride solution were agitated for 24h in a convection oven at the a speed of 150 rpm. pH dependency test was carried out by varying the pH of the solution whereas the isotherm studies were carried out by changing fluoride concentration at three different temperatures. The pH of the fluoride solution were maintained by micro additions of 0.1 NHCl or 0.1 N NaOH. Preliminary desorption test were performed by using HCl, NaCl and NaOH (1 M each) individually at solid liquid ratio of 5 g/L. NaOH solution was found to be effective desorbing solution. Thus optimization desorbing solution for fluoride ion was done by varying the concentration of NaOH solution. The amount of fluoride adsorbed (mg) per unit mass of HTMO precipitates and percentage adsorption of fluoride were determined by using equations as:

$$q = \frac{(C_o - C_e)}{m} \times V \quad \dots \dots (1)$$

$$\%A = \frac{(C_o - C_e)}{C_o} \times 100 \quad \dots \dots (2)$$

where, C_o and C_e are original and final fluoride ion concentration (mg/L), respectively.

The q_e is amount of fluoride ion adsorbed per gram of HTMO precipitates (mg/g), V is volume of the fluoride solution in liter and m is dry weight of HTMO precipitates in gram.

Results and discussion

Characterizations of HTMO precipitate

Figure 1 shows the results of pH drift (equilibrium pH – initial pH) experiment of HTMO precipitate using 0.1M NaCl solution at different pH. The change in pH of the NaCl solution is observed to be zero at pH 6.4, suggesting that the surface of the HTMO precipitate is neutral at this pH and this pH is the pH_{PZC} of instigated HTMO precipitate. The surface of the HTMO precipitate is negative at $pH > pH_{PZC}$ where anion adsorption is not effective whereas its surface is positive at $pH < pH_{PZC}$ which is expected to be favorable condition for approaching anionic species like fluoride anion during adsorption process via electrostatic interaction.

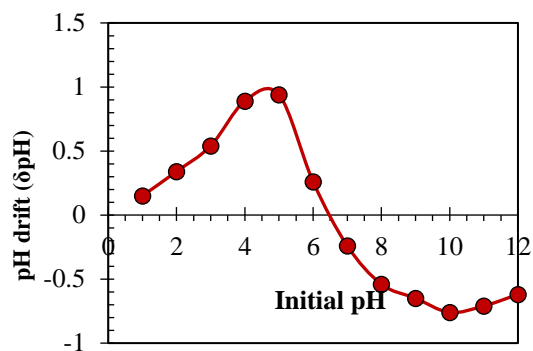


Figure 1: Diagram showing the relationship between pH drift of NaCl solution at different pH after adding HTMO precipitate.

Effect of pH and adsorption mechanism

Speciation of fluoride ions and surface charge of HTMO precipitates varies with pH variation. Due to the increase of proton concentration with increasing acidity of the medium surface of the HTMO precipitates is positive so that adsorption of negatively charged species is more favorable. Majority of fluoride ion exist in the form of fluoride ion at pH higher than 2 whereas it exists as neutral HF and HF_2^- below pH 1.

Figure 2 shows the percentage removal of fluoride using HTMO precipitates at different pH ranging from 1 to 12. It shows that percentage removal of fluoride increases from 94.15 to 99.21% with the increase of equilibrium pH from 1.15 to 2.34. Fluoride removal percentage of HTMO precipitates reached maximum (99.78%) at pH around 6 whereas it is observed to be decreased with further increase of equilibrium pH. HTMO precipitates in aqueous solution have coordinated hydroxyl ion and water ligands. Neutral species of fluoride (HF) predominant at low pH is hardly adsorbed by ion exchange with hydroxyl anion resulting decrease of percentage adsorption of fluoride at low pH. Similarly, the reduction of fluoride removal percentage of HTMO precipitates at basic pH is due to the competition of hydroxyl ions. However, the maximum adsorption of fluoride at pH 2 to 6 can be explained as follows. At acidic pH the hydroxyl ions exist in HTMO precipitates are protonated to give positively charged HTMO surface as depicted in reaction 'a' where interaction of negatively charged species of fluoride is more favored via electrostatic attraction. Similar adsorption behaviors are observed by

Aryal et al., 2022 and Poudel et al., 2021 for the adsorption of metal loaded adsorbents from aqueous medium ^{16, 17}.

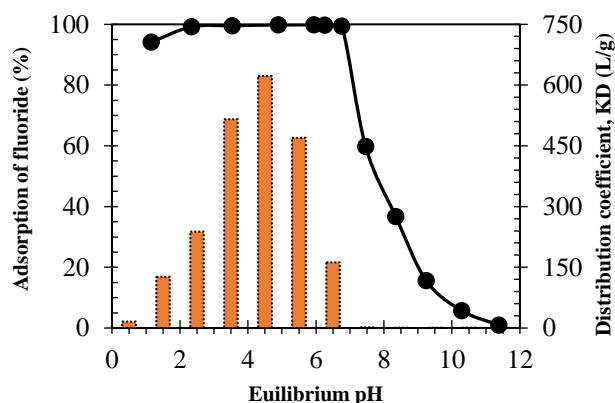
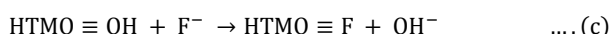


Figure 2: Influence of pH of the solution for the adsorption fluoride onto HTMO adsorbent condition: volume of solution= 10 mL, weight of HTMO = 15 mg, fluoride concentration = 0.5 mmol/L, shaking time = 240 minute, shaking speed = 150 rpm, and temperature = 303K

When fluoride anion approached the protonated HTMO then ion exchange reaction occurred and fluoride ions were adsorbed with the release of water molecule (elementary reaction ‘b’). The proton consumed from the aqueous solution and hydroxyl ion of HTMO gives water molecules. In net reaction, the hydroxyl ligand of HTMO precipitate is exchanged with fluoride ion during adsorption process as shown in reaction ‘c’ as



The distribution ratio is the ratio of the fluoride ion exists in solid adsorbent to the remaining fluoride in the aqueous solution. Distribution coefficient ($K_D = q_e / C_e$) determined at different pH during the adsorption of fluoride onto HTMO precipitate is also presented in Figure 2. The result shows that the distribution coefficient of fluoride in HTMO precipitate is maximum at pH 4.6 thus this pH is confirmed as optimum pH for fluoride ion adsorption.

Effect of contact time

Figure 3 shows the result of fluoride adsorption capacity of in HTMO precipitate as a function of contact time. Fluoride adsorption capacity of HTMO precipitates increase rapidly at the beginning and becomes slower and slower and reached plateau value after 210 minutes. At the start of

experiment, there are comparatively large numbers of active adsorption sites for fluoride ion whereas this number is decreased with time resulting smaller number of active sites available for fluoride ion adsorption. Fluoride uptake capacity increase from 0.067 to 0.38 mmol/g by increasing contact times from 5 minute to 120 minutes. Uptake of fluoride by investigated adsorbent reached 0.43 mmol/g at time 210 minutes whereas it is not higher than 0.44 even after 360 minutes. Therefore, contact time of 210 minute time is optimized for effective adsorption of fluoride ion onto HTMO precipitate. Although adsorption equilibrium was attaining within 210 minute, subsequent adsorption experiment of fluoride was carried out by shaking the solid liquid mixture up to 240 minute (6 hrs) to ensure complete equilibrium.

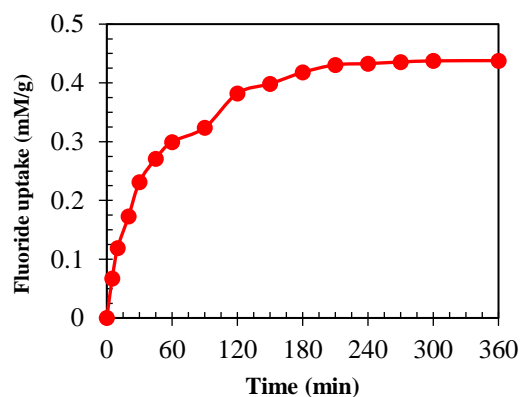


Figure 3: Adsorption kinetics of fluoride ion using HTMO adsorbent condition: volume of solution= 10 mL, weight of HTMO = 15 mg, fluoride concentration = 0.75 mmol/L, pH = 5, and temperature = 303K

The modeling of experimental data is necessary to investigate the best fitted kinetic models thus the experimental data of fluoride adsorption at different times were analyzed using pseudo first order (PFO) model (Eq. 3) and pseudo second (PSO) models (Eq. 4) as ^{18, 19}

$$\log(q_e - q_t) = \log q_e - \frac{k_1}{2.303} t \quad \dots (3)$$

$$\frac{t}{q_t} = \frac{1}{q_e^2 k_2} + \frac{1}{q_e} t \quad \dots (4)$$

where q_e is fluoride uptake capacity of HTMO precipitate and k_1 & k_2 are rate constants for PFO and PSO models, respectively. Pseudo first order rate constant (k_1) and uptake

capacity were determined from the slope and intercept of straight line plot of $\log(q_e - q_t)$ versus time (Figure 4a) whereas that of pseudo second order rate constant and fluoride uptake capacity were determined from intercept and slope of t/q_t versus time plot as shown in Figure 4b.

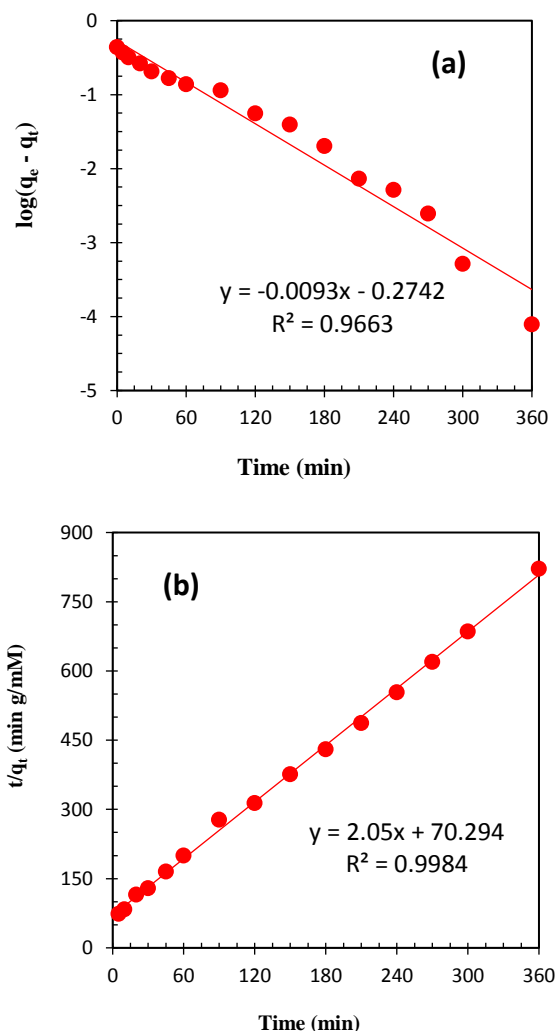


Figure 4: Modeling of kinetic data using (a) pseudo first order (PFO) model and (b) pseudo second order (PSO) model.

All the evaluated values of PFO and PSO kinetics parameters and respective correlation regression coefficient are listed in Table 1.

As can be observed from the results of this table that q_e value evaluated from experiments (0.43 mmol/g) closely resembled with the q_e value determined from PSO model (0.48 mmol/g) but it is higher (0.76 mmol/g) in case of PFO model, indicating that adsorption of fluoride onto HTMO precipitate follows PSO kinetics.

Table 1. Kinetics parameters for the adsorption of fluoride onto HTMO precipitate (RMSE = root mean square error, MAE = Mean average error, χ^2 = Chi-Square)

Kinetic Models	Parameters	Value
Pseudo first order (PFO)	$k_1 \times 10^{-2}$ (min^{-1})	2.14
	q_e , cal. (mmol/g)	0.76
	R^2	0.96
	χ^2	0.14
	RMSE	0.33
Pseudo second order (PSO)	$k_2 \times 10^{-3}$ ($\text{g}/(\text{mg min})$)	0.059
	q_e , cal. (mg/g)	0.48
	R^2	0.99
	q_e , exp. (mg/g)	0.43
	$\chi^2 \times 10^{-3}$	6.85
	RMSE $\times 10^{-2}$	5.78
	MAE $\times 10^{-3}$	3.34

Adsorption isotherm of fluoride

Adsorption isotherm provides the relationship between solid phase concentrations of adsorbate to the liquid phase concentrations at equilibrium. Figure 5 shows the adsorption isotherm of HTMO precipitates for fluoride ion at optimum pH of 5 in three different temperatures. It is clear from the results of this figure that fluoride uptake capacities of HTMO precipitates sharply increased at low concentration and it is gradually increased and reached a plateau value at high concentration. This is the characteristics of Langmuir type adsorption which will be further proved by isotherm modeling.

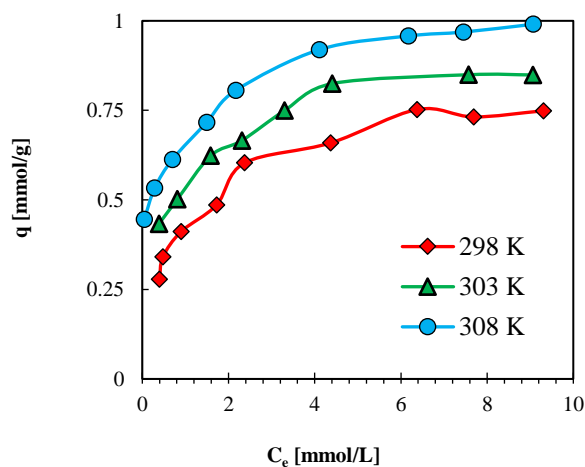


Figure 5: Adsorption isotherm of fluoride using HTMO adsorbent at different temperature condition: volume of solution= 10 mL, weight of HTMO = 15 mg, pH = 5, shaking time = 240 minute, and temperature = 303K.

To find out the best fitted isotherm model and nature of adsorption, the experimental data of fluoride adsorption isotherm is modeled by using Langmuir and Freundlich isotherm models^{20,21}. Langmuir isotherm can be expressed in the non-linear (Eq. 5) and linear form (Eq. 6) as

$$q_e = \frac{q_{\max} b C_e}{1 + b C_e} \quad \dots(5)$$

$$\frac{C_e}{q_e} = \frac{1}{q_{\max} b} + \frac{1}{q_{\max}} C_e \quad \dots(6)$$

where C_e and q_e are the equilibrium concentration of fluoride and uptake capacity at equilibrium, respectively. The constant b (L/mmol) and q_{\max} (mmol/g) are Langmuir equilibrium parameter and maximum adsorption capacity. The Langmuir parameters such as q_{\max} and b are determined from the slope and intercept of the C_e/q_e versus C_e plot (Figure 6a), respectively.

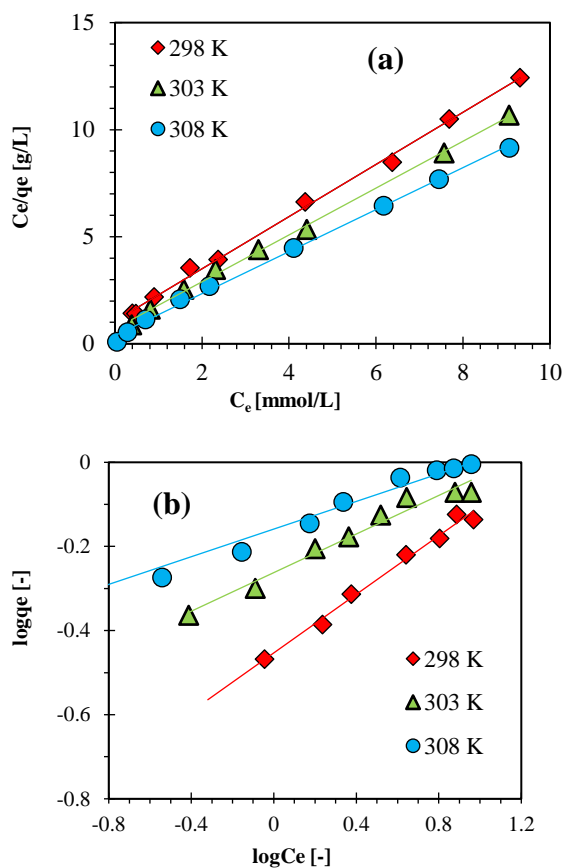


Figure 6: Modeling of isotherm data using (a) Langmuir isotherm and (b) Freundlich isotherm

Similarly, equation 7 (Eq. 7) and 8 (Eq. 8) represents the non-linear and linear form of Freundlich isotherm as

$$q_e = K_F C_e^{\frac{1}{n}} \quad \dots(7)$$

$$\log q_e = \log K_F + \frac{1}{n} \log C_e \dots(8)$$

where K_F and n are Freundlich constant related adsorption potential and intensity of adsorption, respectively. Freundlich isotherms parameters such as n and K_F are estimated from the slope and intercept of $\log q_e$ versus $\log C_e$ plot (Figure 6b). The evaluated values of Langmuir and Freundlich isotherm parameters are listed in Table 2 together with correlation regression coefficients and error functions.

The results of this table shows that the correlation coefficients in case of Langmuir isotherm models is much higher ($R^2 > 0.99$) and close to unity whereas its value is small in case of Freundlich isotherm model (only $R^2 < 0.96$). The maximum adsorption capacity of investigated HTMO precipitates for fluoride was found as 0.83, 0.92, 1.02 mmol/g at 298, 303 and 308K, respectively.

Table 2. Isotherm parameters for the adsorption of fluoride onto HTMO precipitate

Isotherm parameters		298K	303K	308K
Langmuir isotherm	q_{exp} (mmol/g)	0.75	0.84	0.97
	q_m (mmol/g)	0.83	0.92	1.02
	b (L/mmol)	1.13	1.55	2.58
	R^2	0.99	0.99	0.99
	$\chi^2 \times 10^{-2}$	0.77	0.69	0.24
	RMSE $\times 10^{-2}$	0.64	0.64	0.25
MAE	0.08	0.08	0.05	
Freundlich isotherm	K_F (mmol/g) (L/mmol) ^{1/n}	0.63	0.76	0.85
	1/n	0.34	0.23	0.16
	R^2	0.98	0.96	0.97
	$\chi^2 \times 10^{-2}$	2.05	0.64	1.09
	RMSE $\times 10^{-2}$	1.30	0.49	0.93
	MAE	0.11	0.07	0.09

Furthermore; the values of correlation coefficient (R^2) is high and error function such as Chai square (χ^2), root mean

square error (RMSE) and mean average error (MAE) are small in case of Langmuir isotherm model (also shown in Table 2) compared to Freundlich isotherm model suggesting better fitting of experimental data with Langmuir isotherm model.

To make the better understanding, the maximum adsorption capacity of investigated HTMO is compared with the similar metal oxide-based adsorbent reported in the literature as shown in the Table 3²²⁻³². It is clear from the results of this Table that the Fe (III)-Al (III)-Ce (IV) adsorbents containing tetravalent Ce (IV) possess highest adsorption capacity then other adsorbents which may be due to very high affinity of Ce (IV) with fluoride ion. Moreover, the fluoride adsorption capacity of investigated HTMO is satisfactory, suggesting that it can be a promising material for the removal of fluoride from contaminated water.

Table 3. Comparison of maximum adsorption capacities of different reported adsorbents with investigated HTMO

Adsorbents	q _{max} (mmol/g)	pH	References
HTMO precipitate	1.02	6	This study
Hydrous ferrous oxide	1.80	4	22
Fe(II)-Al(III)-Ce(IV) adsorbent	9.36	7	23
Fe-Al-Ce oxide coated sand	0.18	7	24
Glass bead sprayed with Fe-Al-Ce	0.31	7	25
Granular ferric hydroxide	0.37	4	26
Fe-Sn bimetal oxide adsorbent	0.55	7	27
Fe(II)-Ti(IV) nano adsorbent	2.47	-	28
F(III)-Cr(III) mixed oxide	0.86	3	29
Al/Fe impregnated granular ceramics	0.19	4	30
Fe ₂ O ₄ /Al ₂ O ₃ nanoparticle	3.68	7	31
Al/Fe dispersed ceramics	0.09	6	32

Thermodynamic study

Thermodynamic property of the system is related to the equilibrium constant. The equilibrium constant can be

determined from Langmuir equilibrium parameter (b, L/mmol). The equilibrium constant is dimensionless parameter but Langmuir equilibrium parameter b in this study has the unit of liter per milimole. As experiment is carried out in aqueous medium so that mole of water (55.6mol/L) should be multiply with Langmuir equilibrium parameter to obtain the exact equilibrium constant as^{33, 34}

$$K_C = b \times M_{H_2O} \times 1000 \quad \dots (9)$$

Gibbs free energy change of the system at standard state (ΔG°) is related to equilibrium constant as

$$\Delta G^\circ = -RT \ln K_C \quad \dots (10)$$

Gibb's free energy change, entropy change, and enthalpy change are related by the equation as:

$$\Delta G^\circ = \Delta H^\circ - T \Delta S^\circ \quad \dots (11)$$

From equation (10) and (11) we have

$$\ln K_C = \frac{\Delta H^\circ}{RT} + \frac{\Delta S^\circ}{R} \quad \dots (12)$$

where, ΔH° and ΔS° are standard enthalpy and entropy change, respectively.

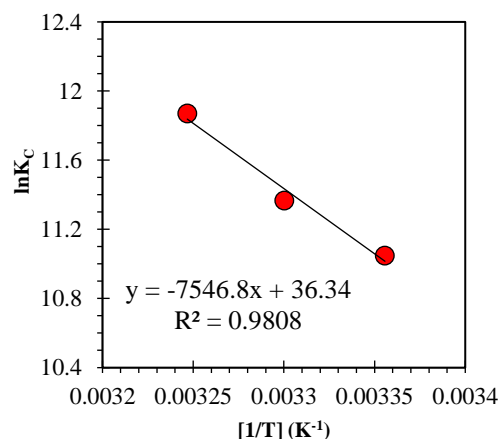


Figure 7: Vent Hoff's plot for the evaluation of thermodynamic parameters.

Table4. Evaluated thermodynamic parameters for fluoride adsorption onto HTMO precipitate

Temp. (K)	K _C	ΔG° (kJ/mol)	ΔH° (kJ/mol)	ΔS° (kJ/mol K)
308	62830.18	-0.308		
303	86421.42	-0.312	62.74	0.31
298	143131.57	-0.320		

Figure 7 shows the Vents Hoff's plots for the adsorption of fluoride onto HTMO precipitates. The values of ΔG° at different temperatures are calculated directly using equation 8 (Eq. 8) whereas that of values were ΔH° and ΔS°

are evaluated slope and intercept of Vent Hoff's plots of $\ln K_c$ versus $1/T$, respectively. All the thermodynamic parameters evaluated for the adsorption of fluoride onto HTMO precipitates are shown in Table 4. It shows that the negative value of ΔG° increases with increasing temperature suggesting spontaneous and endothermic reaction. Estimated value of positive ΔH° (62.74 kJ/mol) confirms the endothermic nature of fluoride adsorption onto investigated HTMO precipitates.

Desorption of fluoride ion

Preliminary desorption experiments is carried out by using HCl, NaCl and NaOH (1M each) solution at 10 g/L solid liquid ratio to investigate the nature of desorbing solution. From this it was found that NaCl, HCl and NaOH desorbed 21.48%, 89.37% and 98.82% fluoride from fluoride loaded HTMO precipitates. NaCl is not effective for desorption of fluoride, HCl could effectively desorbs fluoride but invites the trouble dissolving HTMO precipitates. NaOH successfully desorbed more than 98% of loaded fluoride without deterioration of active sites thus optimization of desorbing solution was done by varying the concentration of NaOH. Figure 8 shows the percentage desorption of fluoride from fluoride loaded HTMO precipitates using different concentration of NaOH ranging from 0.01 to 0.75M at solid liquid ratio of 5 g/L.

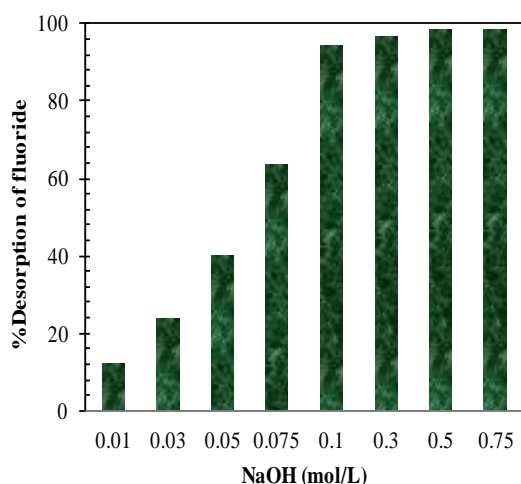


Figure 8: Desorption of adsorbed fluoride from fluoride loaded HTMO using alkali solution condition: volume of NaOH = 10 mL, weight of fluoride loaded HTMO = 50 mg, fluoride in fluoride loaded HTMO = 0.23 mmol/g, shaking time = 240 minute, shaking speed = 150 rpm, and temperature = 303K.

It is evident from the result of this figure that desorption of fluoride increased from 12.36% to 94.56% with the increase of NaOH concentration from 0.01 to 0.1M. After that desorption percentage is insignificantly increased and reached only 98.67% by using 0.75M NaOH. Therefore 0.1M NaOH is optimized for the effective desorption of fluoride from fluoride loaded HTMO precipitates.

It is inferred that the fluoride from fluoride loaded HTMO precipitates is desorbed by ligand exchange reaction with hydroxyl ion provided from desorbing solution of NaOH as depicted by elementary reaction 'd'. Number of available hydroxyl ion increased with the increase of NaOH concentration that probably increase the probability of ligand exchange reaction with adsorbed fluoride ion in fluoride loaded HTMO precipitate resulting higher desorption percentage at elevated concentration of NaOH. The behavior is exactly similar to other reported adsorbents^{35,36}.



Conclusion

To summarize, we have investigated metal oxide based HTMO precipitate for the removal of fluoride from water. A batch study was conducted to get information on effect of pH, contact time, concentration and temperature for the removal of fluoride ions. Fluoride removal by HTMO precipitate was found to be significantly influenced by pH of the solution and maximum adsorption occurred at pH 6. The rate of adsorption was found to be fast and equilibrium was reached within 210 minutes. We found maximum adsorption capacity of HTMO precipitate for fluoride is 0.83, 0.92, 1.02 mmol/g at 298, 303 and 308K, respectively. Thermodynamic study suggested that adsorption of fluoride onto HTMO precipitate is spontaneous (negative ΔG° value) and endothermic (positive ΔH° value). The adsorbed fluoride from fluoride loaded HTMO precipitate could be done using 0.1 M NaOH solutions. Thus the HTMO precipitate investigated in this study can be an effective and high capacity metal oxide based adsorbent for the treatment of water polluted with fluoride ion.

References

1. Bibi, S., Farooqi, A., Yasmin, A., Kamran, M. A. and Niazi, N. K. 2017. Arsenic and fluoride removal by potato peel and rice husk (PPRH) ash in aqueous environments. *International Journal of Phytoremediation*. **19(11)**:1029–1036. <https://doi.org/10.1080/15226514.2017.1319329>
2. Biswas, G., Kumari, M., Adhikari, K. and Dutta, S. 2017. Application of response surface methodology for optimization of biosorption of fluoride from groundwater using *Shorea robusta* flower petal. *Applied Water Science*. **7(8)**:4673–4690. <https://doi.org/10.1007/s13201-017-0630-5>
3. Tan, T. L., Krusnamurthy, P. A., Nakajima, H. and Rashid, S. A. 2020. Adsorptive, kinetics and regeneration studies of fluoride removal from water using zirconium-based metal organic frameworks. *RSC Advances*. **10(32)**: 18740–18752. <https://doi.org/10.1039/d0ra01268h>
4. Paudyal, H., Pangeni, B., Inoue, K., Kawakita, H., Ohto, K., Harada, H. and Alam, S. 2011. Adsorptive removal of fluoride from aqueous solution using orange waste loaded with multi-valent metal ions. *Journal of Hazardous Materials*. **192(2)**: 676–682. <https://doi.org/10.1016/j.jhazmat.2011.05.070>
5. WHO, 2008. Guidelines for Drinking-water Quality: fourth edition incorporating the first addendum, Geneva.
6. Solanki, Y. S., Agarwal, M., Maheshwari, K., Gupta, S., Shukla, P. and Gupta, A. B. 2021. Removal of fluoride from water by using a coagulant (inorganic polymeric coagulant). *Environmental Science and Pollution Research*. **28(4)**: 3897–3905. <https://doi.org/10.1007/s11356-020-09579-2>
7. Tomonori, K. 2018. De-fluoridation of drinking water by coprecipitation with magnesium hydroxide in electrolysis. *Cogent Engineering*. **5(1)**: 1558498. <https://doi.org/10.1080/23311916.2018.1558498>
8. Owusu-Agyeman, I., Reinwald, M., Jehanipour, A. and Schäfer, A. I. 2019. Removal of fluoride and natural organic matter removal from natural tropical brackish waters by nanofiltration/reverse osmosis with varying water chemistry. *Chemosphere*. **217**: 47–58. <https://doi.org/10.1016/j.chemosphere.2018.10.135>
9. Djouadi Belkada, F., Kitous, O., Drouiche, N., Aoudj, S., Bouchelaghem, O., Abdi, N., Grib, H. and Mameri, N. 2018. Electrodialysis for fluoride and nitrate removal from synthesized photovoltaic industry wastewater. *Separation and Purification Technology*. **204**: 108–115. <https://doi.org/10.1016/j.seppur.2018.04.068>
10. Grzegorzec, M., Majewska-Nowak, K. and Ahmed, A. E. 2020. Removal of fluoride from multicomponent water solutions with the use of monovalent selective ion-exchange membranes. *Science of the Total Environment*. **722**: 137681. <https://doi.org/10.1016/j.scitotenv.2020.137681>
11. Xu, L., Chen, G., Peng, C., Qiao, H., Ke, F., Hou, R., Li, D. and Wan, X. 2017. Adsorptive removal of fluoride from drinking water using porous starch loaded with common metal ions. *Carbohydrate Polymers*. **160**: 82–89. <https://doi.org/10.1016/j.carbpol.2016.12.052>
12. Zirpe, M., Bagla, H. and Thakur, J. 2020. Adsorptive removal of fluoride using polymer-modified ceria nanoparticles: determination of equilibrium, kinetic and thermodynamic parameters. *Separation Science and Technology (Philadelphia)*. **55(16)**: 2933–2947. <https://doi.org/10.1080/01496395.2019.1660674>
13. Takmil, F., Esmaili, H., Mousavi, S. M. and Hashemi, S. A. 2020. Nano-magnetically modified activated carbon prepared by oak shell for treatment of wastewater containing fluoride ion. *Advanced Powder Technology*. **31(8)**: 3236–3245. <https://doi.org/10.1016/j.apt.2020.06.015>
14. Siddique, A., Nayak, A. K. and Singh, J. 2020. Synthesis of FeCl₃-activated carbon derived from waste citrus limetta peels for removal of fluoride: an eco-friendly approach for the treatment of groundwater and bio-waste collectively. *Groundwater for Sustainable Development*. **10**: 100339. <https://doi.org/10.1016/j.gsd.2020.100339>
15. Poudel, B. R., Aryal, R. L., Gautam, S. K., Ghimire, K. N., Paudyal, H. and Pokhrel, M. R. 2021. Effective remediation of arsenate from contaminated water by zirconium modified pomegranate peel as an anion exchanger. *Journal of Environmental Chemical Engineering*. **9(6)**: 106552. <https://doi.org/10.1016/j.jece.2021.106552>
16. Aryal, R.L., Poudel, B.R., Pokhrel, M.R., Paudyal, H. and Ghimire, K.N. 2021. Sequestration of phosphate from water onto modified watermelon waste loaded with Zr(IV). *Separation Science and Technology*. **57(1)**:1-13. <https://doi.org/10.1080/01496395.2021.1884878>
17. Paudyal, H., Pangeni, B., Ghimire, K.N., Inoue, K., Kawakita, H., Ohto, K. and Alam, S. 2012. Adsorption behavior of orange waste gel for some rare earth ions and its application to the removal of fluoride from water. *Chemical Engineering Journal*. **195(196)**: 289–296. <https://doi.org/10.1016/j.cej.2012.04.061>
18. Lagergren, S. 1998. Zurtheorie der sogenannten adsorption geloesterstoffe, *Veternskapskad. Handl.* **24**: 1-39.
19. Blanchanchard, G., Maunaye, M. and Marti, G. 1984. Removal of heavy metal from water by means of natural zeolites. *Water Research*. **18(2)**:1501 -1507.
20. Langmuir, I. 1916. The constitution and fundamental properties of solids and liquids. *Journal of American Chemical Society*. **38(1916)**: 2221–2295. <https://doi.org/10.1021/ja02268a002>
21. Freundlich, H. 1906. Über die adsorption in losungen. *Journal of Physical Chem. try*. **57**:385 – 470.
22. Streat, M., Hellgardt, K. and Newton, N.L.R. 2008. Hydrous ferric oxide as an adsorbent in water treatment: batch and mini-column adsorption of arsenic, phosphorus, fluorine and cadmium ions. *Process Safety and Environmental Protection*. **86(1)**: 21–30. <https://doi.org/10.1016/j.psep.2007.10.009>
23. Wu, X., Zhang, Y., Dou, X. and Yang, M. 2007. Fluoride removal performance of a novel Fe–Al–Ce trimetal oxide adsorbent. *Chemosphere*. **69 (11)**: 1758–1764. <http://doi.org/10.1016/j.chemosphere.2007.05.075>
24. Wu, H.X., Wang, T.J., Dou, X.M., Zhao, B., Chen, L. and Jin, Y. 2008. Spray coating of adsorbent with polymer latex on sand particles for

- fluoride removal in drinking water. *Industrial and Engineering Chemistry Research*. **47(14)**:4697–4702.
<https://doi.org/10.1021/ie800278b>
25. Chen, L., Wang, T.J., Wu, H.X., Jin, Y., Zhang, Y., and Dou X.M. 2011. Optimization of a Fe–Al–Ce nano-adsorbent granulation process that used spray coating in a fluidized bed for fluoride removal from drinking water. *Powder Technology*. **206(3)**: 291–296.
<https://doi.org/10.1016/j.powtec.2009.02.007>
26. Kumar, E., Bhatnagar, A., Minkyu, J., Jung, W., Lee, S., Kim, S., Lee, G., Song, H., Choi, J., Yang, J. and Jeon, B. 2009. Defluoridation from aqueous solutions by granular ferric hydroxide (GFH). *Water Research*. **43(2)**: 490–499.
<https://doi.org/10.1016/j.watres.2008.10.031>
27. Biswas, K., Gupta, K. and Ghosh, U.C. 2009. Adsorption of fluoride by hydrous iron (III)- tin (IV) bimetal Mixed oxide from the aqueous solutions. *Chemical Engineering Journal*. **49**: 96–206.
<https://doi.org/10.1016/j.cej.2008.09.047>
28. Chen, L., He, B.Y., He, S., Wang, T.J., Su, C.L. and Jin, Y. 2012. Fe–Ti oxide nano-adsorbent synthesized by co-precipitation for fluoride removal from drinking water and its adsorption mechanism. *Powder Technology*. **227**: 3–8. <https://doi.org/10.1016/j.powtec.2011.11.030>
29. Biswas, K., Debnath, S. and Ghosh, U.C. 2010. Physicochemical aspects on fluoride adsorption for removal from water by synthetic hydrous Iron(III) –Chromium (III) mixed oxide. *Separation Science and Technology*. **45**: 472–485.
<https://doi.org/10.1080/01496390903526667>
30. Chen, N., Feng, C., Miao, L. 2014. Fluoride removal on Fe–Al-impregnated granular ceramic adsorbent from aqueous solution. *Clean Technology and Environmental Policy*. **16(3)**:609-617.
[doi10.1007/s10098-013-0659-6](https://doi.org/10.1007/s10098-013-0659-6)
31. Chai, L., Wang, Y., Zhao, N., Yang, W. and You, X. 2013. Sulfate-doped Fe₃O₄/Al₂O₃ nanoparticles as a novel adsorbent for fluoride removal from drinking water. *Water Research*. **47(12)**: 4040–4049.
<https://doi.org/10.1016/j.watres.2013.02.057>
32. Chen, N., Zhang, Z., Feng, C., Zhu, D., Yang, Y. and Sugiura, N. 2011. Preparation and characterization of porous granular ceramic containing dispersed aluminum and iron oxides as adsorbents for fluoride removal from aqueous solution. *Journal of Hazardous Materials*. **186(1)**: 863–868.
<https://doi.org/10.1016/j.jhazmat.2010.11.083>
33. Zhou, X. and Zhou, X. 2014. The unit problem in the thermodynamic calculation of adsorption using langmuir equation. *Chemical Engineering and Communication*. **201**: 1459–1467.
<https://doi.org/10.1080/00986445.2013.818541>
34. Xu, L., et al. 2021. Selective adsorption of Pb²⁺ and Cu²⁺ on amino-modified attapulgite: kinetic, thermal dynamic and DFT studies. *Journal of Hazardous Materials*. **404**: 124140.
<https://doi.org/10.1016/j.jhazmat.2020.124140>
35. Paudyal, H., Inoue, K., Kawakita, H., Ohto, K., Kamata. H. and Alam, S. 2020. Recovery of fluoride from water through adsorption using orange–waste gel, followed by desorption using saturated lime water. *Journal of Material Cycles Waste Management*. **22**:1484–1491.
<https://doi.org/10.1007/s10163-020-01042-1>
36. Paudyal, H., Pangen, B., Inoue, K., Harada, H., Kawakita, H., Ohto, K. and Alam, S. 2017. Adsorptive removal of trace concentration of fluoride using orange waste treated using concentrated sulphuric acid. *International Journal of Materials Science and Applications*. **6(4)**: 212-221. <http://www.sciencepublishinggroup.com/j/ijmsa>